

# Alkaline Earth Complexes of 1,4,7,10-Tetrakis(2-hydroxyethyl)- and 1,4,7,10-Tetrakis(2-methoxyethyl)-1,4,7,10-tetraazacyclododecane: An Equilibrium and Kinetic Study

Ramesh Dhillon,<sup>†</sup> Stephen F. Lincoln,<sup>\*,†,‡</sup> Samer Madbak,<sup>†</sup> Ashley K. W. Stephens,<sup>†</sup> Kevin P. Wainwright,<sup>§</sup> and Sonya L. Whitbread<sup>†</sup>

Departments of Chemistry, University of Adelaide, Adelaide, SA 5005, Australia, and The Flinders University of South Australia, Adelaide, GPO Box 2100, SA 5001, Australia

Received June 2, 1999

The 1,4,7,10-tetrakis(2-hydroxyethyl)-1,4,7,10-tetraazacyclododecane complexes  $[M(\text{thec12})]^{2+}$ , where  $M^{2+} = \text{Mg}^{2+}$ ,  $\text{Ca}^{2+}$ ,  $\text{Sr}^{2+}$ , and  $\text{Ba}^{2+}$ , are characterized by  $\log(K/\text{dm}^3 \text{ mol}^{-1}) = 2.86 \pm 0.09$ ,  $7.41 \pm 0.04$ ,  $6.47 \pm 0.04$ , and  $4.84 \pm 0.03$  at 298.2 K in aqueous  $\text{Et}_4\text{NClO}_4$  ( $I = 0.10 \text{ mol dm}^{-3}$ ), where  $K$  is a potentiometrically determined stability constant. The analogous literature values for the 1,4,7,10-tetrakis(2-methoxyethyl)-1,4,7,10-tetraazacyclododecane complexes  $[M(\text{tmec12})]^{2+}$  are 2.47, 5.47, 5.00, and 4.72. The enantiomerization of eight-coordinate  $\Delta$ - and  $\Lambda$ - $[M(\text{thec12})]^{2+}$  is characterized by  $k(298.2 \text{ K}) = 2310 \pm 260$ ,  $582 \pm 17$ , and  $445 \pm 5 \text{ s}^{-1}$ ,  $\Delta H^\ddagger = 19.1 \pm 0.8$ ,  $33.3 \pm 0.5$ , and  $43.9 \pm 0.4 \text{ kJ mol}^{-1}$ , and  $\Delta S^\ddagger = -117 \pm 4$ ,  $-80.3 \pm 1.8$ , and  $-47.0 \pm 1.3 \text{ J K}^{-1} \text{ mol}^{-1}$  when  $M^{2+} = \text{Mg}^{2+}$ ,  $\text{Ca}^{2+}$ , and  $\text{Ba}^{2+}$ , respectively, in methanol- $^{12}\text{C}$ - $d_4$  as shown by  $^{13}\text{C}$  NMR spectroscopy. For the enantiomerization of eight-coordinate  $\Delta$ - and  $\Lambda$ - $[M(\text{tmec12})]^{2+}$ ,  $k(298.2 \text{ K}) = 310 \pm 1$  and  $688 \pm 3 \text{ s}^{-1}$ ,  $\Delta H^\ddagger = 54.0 \pm 0.2$  and  $39.6 \pm 0.1 \text{ kJ mol}^{-1}$ , and  $\Delta S^\ddagger = -16.1 \pm 0.5$  and  $-57.9 \pm 0.3 \text{ J K}^{-1} \text{ mol}^{-1}$  when  $M^{2+} = \text{Ca}^{2+}$  and  $\text{Ba}^{2+}$ , respectively. However,  $[\text{Mg}(\text{tmec12})]^{2+}$  has a seven-coordinate structure where one of the methoxy groups is not coordinated and exchange of the methoxy groups between the coordinated and free states is characterized by  $k(298.2 \text{ K}) = 163\,000 \pm 8000 \text{ s}^{-1}$ ,  $\Delta H^\ddagger = 35.8 \pm 0.4 \text{ kJ mol}^{-1}$ , and  $\Delta S^\ddagger = -25.1 \pm 1.7 \text{ J K}^{-1} \text{ mol}^{-1}$ . The intermolecular exchange of thec12 and tmec12 between the coordinated and free states is substantially slower than the enantiomerizations in the first five complexes and the intramolecular exchange process observed in  $[\text{Mg}(\text{tmec12})]^{2+}$ .

## Introduction

The pendant arm macrocycles 1,4,7,10-tetrakis(2-hydroxyethyl)- and 1,4,7,10-tetrakis(2-methoxyethyl)-1,4,7,10-tetraazacyclododecane, thec12 and tmec12, respectively, are potentially octadentate ligands (Figure 1). However, in the solid state thec12 is penta-, hepta-, and octadentate in  $[\text{Li}(\text{thec12})]^+$ ,  $[\text{Na}(\text{thec12})]^+$ , and  $[\text{K}(\text{thec12})]^+$ , respectively, where in each case the metal center lies above the plane of the four coordinated nitrogens.<sup>1–3</sup> In  $[\text{K}(\text{thec12})]^+$  the coordinated atoms are at the corners of a cube where the plane of the four oxygens is twisted about the  $C_4$  axis with respect to the four nitrogen plane. In methanol- $^{12}\text{C}$ - $d_4$ ,  $^{13}\text{C}$  NMR spectroscopy shows all four pendant arms of thec12 in these complexes to be equivalent consistent with the assumption of eight-coordinate structures similar to that of  $[\text{K}(\text{thec12})]^+$  in the solid state.<sup>4</sup> The  $[\text{M}(\text{tmec12})]^+$  analogues are also eight-coordinate in methanol- $^{12}\text{C}$ - $d_4$ .<sup>5,6</sup> We are interested in the factors affecting ligand denticity, stereo-

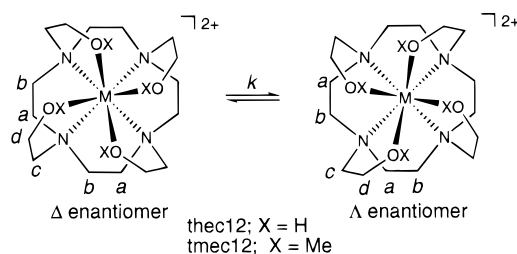


**Figure 1.** Scheme showing structures and enantiomerization of  $\Delta[M(\text{thec12})]^{2+}$  and  $\Lambda[M(\text{thec12})]^{2+}$  ( $R = \text{H}$ ) and of  $\Delta-[M(\text{tmec12})]^{2+}$  and  $\Lambda-[M(\text{tmec12})]^{2+}$  ( $R = \text{Me}$ ). When viewed down the  $C_4$  axis from the oxygen plane, the enantiomer in which that plane is twisted to the right with respect to the nitrogen plane is designated  $\Delta$ . The twist is to the left for the  $\Lambda$  enantiomer. The twist angles are exaggerated for illustrative purposes.

chemistry, and lability in thec12 and tmec12 metal complexes out of intrinsic interest and also because thec12 is one of the basic ligands on which we are seeking to build molecular receptor sites.<sup>7,8</sup> Because of their systematic change in ionic radii, we selected the alkaline earth ions for study of the coordinating characteristics of thec12 and tmec12 with divalent metal ions. We find that both ligands are octadentate in their

<sup>†</sup> University of Adelaide.

<sup>‡</sup> E-mail: Stephen.Lincoln@adelaide.edu.au.

<sup>§</sup> The Flinders University of South Australia.

- (1) Buøen, S.; Dale, J.; Groth, P.; Krane, J. *J. Chem. Soc., Chem. Commun.* **1982**, 1172–1174.
- (2) Groth, P. *Acta Chem. Scand. A* **1983**, *37*, 71–74.
- (3) Groth, P. *Acta Chem. Scand. A* **1983**, *37*, 283–291.
- (4) Whitbread, S. L.; Politis, S.; Stephens, A. K. W.; Lucas, J. B.; Dhillon, R. S.; Lincoln, S. F.; Wainwright, K. P. *J. Chem. Soc., Dalton Trans.* **1996**, 1379–1384.
- (5) Stephens, A. K. W.; Dhillon, R. S.; Madbak, S. E.; Whitbread, S. L.; Lincoln, S. F. *Inorg. Chem.* **1996**, *35*, 2019–2024.
- (6) Lincoln, S. F. *Coord. Chem. Rev.* **1997**, *166*, 255–289.

(7) Whitbread, S. L.; Valente, P.; Buntine, M. A.; Clements, P.; Lincoln, S. F.; Wainwright, K. P. *J. Am. Chem. Soc.* **1998**, *120*, 2862–2869, 11212.

(8) Smith, C. B.; Wallwork, K. S.; Weeks, J. M.; Buntine, M. A.; Lincoln, S. F.; Taylor, M. R.; Wainwright, K. P. *Inorg. Chem.* **1999**, *38*, 4986–4992.

Mg<sup>2+</sup>, Ca<sup>2+</sup>, and Ba<sup>2+</sup> complexes in methanol-<sup>12</sup>C-*d*<sub>4</sub> (with the exception of [Mg(tmec12)]<sup>2+</sup> where tmec is heptadentate) and that the complexes undergo enantiomerization (Figure 1) at rates within the <sup>13</sup>C NMR time scale.

### Experimental Section

The preparations of thec12 and tmec12 were as described in the literature.<sup>1,9,10</sup> The alkaline earth triflates were prepared by adding a small excess of the alkaline earth carbonate slowly to 98% CF<sub>3</sub>SO<sub>3</sub>H (Aldrich) with stirring followed by stirring for 2 days. The excess carbonate was filtered off, and concentration produced white crystalline alkaline earth triflates that were twice recrystallized from water. Tetraethylammonium perchlorate was prepared by precipitation from aqueous NEt<sub>4</sub>Br (BDH) solution with excess HClO<sub>4</sub> and was recrystallized from water until no acid or bromide was detectable. All of the salts were dried to constant weight over P<sub>2</sub>O<sub>5</sub> under vacuum at 353–363 K for 48 h and were stored over P<sub>2</sub>O<sub>5</sub> under vacuum at room temperature. (**Caution!** *Anhydrous perchlorate salts are potentially powerful oxidants and should be handled with care.*)

Deionized water, purified with a MilliQ-Reagent system to give a specific resistance of > 15 MΩ cm, which was subsequently boiled to remove CO<sub>2</sub>, was used to prepare solutions for potentiometric titration. A Metrohm Dosimat E665 titrator, an Orion SA 720 potentiometer, and an Orion 8172 Ross Sureflow combination pH electrode filled with 0.10 mol dm<sup>-3</sup> NEt<sub>4</sub>ClO<sub>4</sub> were used in all titrations. During each titration a fine stream of nitrogen bubbles (previously passed through aqueous 0.10 mol dm<sup>-3</sup> NEt<sub>4</sub>OH (Aldrich) to remove any CO<sub>2</sub> traces and then through aqueous 0.10 mol dm<sup>-3</sup> NEt<sub>4</sub>ClO<sub>4</sub>) was passed through the titration solution that was magnetically stirred and thermostated at 298.2 ± 0.1 K in a water-jacketed 20 cm<sup>3</sup> titration vessel that was closed with the exception of a small vent for the nitrogen stream. The electrode was calibrated by titration of 0.100 mol dm<sup>-3</sup> NEt<sub>4</sub>OH from the autoburet against 0.005 mol dm<sup>-3</sup> HClO<sub>4</sub> (10.00 cm<sup>3</sup>). The pK<sub>a</sub>s of triprotonated thec12 were determined from titrations of solutions (10.00 cm<sup>3</sup>) 0.005 and 0.001 mol dm<sup>-3</sup> in HClO<sub>4</sub> and thec12, respectively, against 0.100 mol dm<sup>-3</sup> NEt<sub>4</sub>OH. The [M(thec12)]<sup>2+</sup> stability constants were determined from titrations of solutions (10.00 cm<sup>3</sup>) 0.005, 0.001, and 0.0005–0.0020 in HClO<sub>4</sub>, thec12, and M(ClO<sub>4</sub>)<sub>2</sub>, respectively, against 0.100 mol dm<sup>-3</sup> NEt<sub>4</sub>OH. Prior to titration, each solution was allowed at least 30 min to reach thermal equilibrium in the titration vessel. All titrations were carried out in triplicate at least. The pK<sub>a</sub>s of triprotonated thec12 and the stability constants of [M(thec12)]<sup>2+</sup> were derived from the titration data using the program SUPERQUAD.<sup>11</sup>

In the NMR experiments, methanol-<sup>12</sup>C-*d*<sub>4</sub> (99.95 atom % <sup>12</sup>C and 99.5% <sup>2</sup>H, Aldrich) was used as received. Solutions of alkaline earth triflates and either thec12 or tmec12 of the desired mole ratio were prepared by weight under dry nitrogen in a glovebox and were transferred to tightly stoppered 5-mm NMR tubes. Carbon-13 (broadband <sup>1</sup>H decoupled) NMR spectra were run at 75.47 MHz on a Bruker CXP-300 spectrometer, and 6000 transients were accumulated in a 8192 data point base over a 3000 Hz spectral width for each solution prior to Fourier transformation. The solution temperature was controlled to within ±0.3 K using a Bruker B-VT 1000 temperature controller. The Fourier transformed spectra were subjected to complete line shape analysis<sup>12</sup> on a VAX 11-780 computer to obtain rate parameters. The temperature-dependent <sup>13</sup>C line widths and chemical shifts employed in the analysis were obtained by extrapolation from low temperatures where no exchange-induced modification occurred.

### Results and Discussion

**Complex Stability.** In aqueous solution the magnitude of the [M(thec12)]<sup>2+</sup> stability constant, *K* (= [M(thec12)]<sup>2+</sup>/

**Table 1.** Stability Constants for [M(thec12)]<sup>2+</sup> and [M(tmec12)]<sup>2+</sup> in Water at *I* = 0.10 mol dm<sup>-3</sup> (Et<sub>4</sub>NClO<sub>4</sub>) at 298.2 K

M <sup>2+</sup>	log( <i>K</i> /dm <sup>3</sup> mol <sup>-1</sup> )	
	[M(thec12)] <sup>2+</sup>	[M(tmec12)] <sup>2+</sup> <sup>b</sup>
Mg <sup>2+</sup> (89 pm) <sup>a</sup>	2.86 ± 0.09	2.47 ± 0.05
Ca <sup>2+</sup> (112 pm) <sup>a</sup>	7.41 ± 0.04	5.47 ± 0.05
Sr <sup>2+</sup> (126 pm) <sup>a</sup>	6.47 ± 0.04	5.00 ± 0.05
Ba <sup>2+</sup> (142 pm) <sup>a</sup>	4.84 ± 0.03	4.72 ± 0.05

<sup>a</sup> 8-coordinate ionic radii from ref 14. <sup>b</sup> From ref 9. The pK<sub>a</sub>s of triprotonated thec12 were determined to be 1.94 ± 0.07, 8.16 ± 0.05, and 10.74 ± 0.05, and those for triprotonated tmec12 are 2.17, 8.04, and 10.92 as reported in ref 9.

([M<sup>2+</sup>][thec12]), varies with M<sup>2+</sup> in the sequence Mg<sup>2+</sup> < Ca<sup>2+</sup> > Sr<sup>2+</sup> > Ba<sup>2+</sup>, and similar variations are observed for [M(tmec12)]<sup>2+</sup> (Table 1). These variations in stability reflect a balance among (i) the hydration energy of M<sup>2+</sup>, (ii) the electron pair donating power of the ligand, and (iii) the ability of the ligand to assume a stereochemistry that optimizes bonding with M<sup>2+</sup>. The hydration energies (parenthetical figures in kJ mol<sup>-1</sup>)<sup>13</sup> decrease in the sequence Mg<sup>2+</sup> (1922), Ca<sup>2+</sup> (1592), Sr<sup>2+</sup> (1445), and Ba<sup>2+</sup> (1304) as the ionic radii<sup>14</sup> increase from Mg<sup>2+</sup> to Ba<sup>2+</sup> (Table 1). The balance among i–iii most favoring complexation is achieved with Ca<sup>2+</sup> for both for [M(thec12)]<sup>2+</sup> and [M(tmec12)]<sup>2+</sup> as indicated by the largest log(*K*/dm<sup>3</sup> mol<sup>-1</sup>) in each series. The difference in stability between the Mg<sup>2+</sup> and Ca<sup>2+</sup> complexes is particularly great as is the difference in ionic radii between Mg<sup>2+</sup> and Ca<sup>2+</sup>. This may reflect steric crowding about the smaller Mg<sup>2+</sup>. Steric crowding by the methyl groups of tmec12 may also explain the generally lower stabilities of [M(tmec12)]<sup>2+</sup>, by comparison with those of [M(thec12)]<sup>2+</sup> for M<sup>2+</sup> = Mg<sup>2+</sup>, Ca<sup>2+</sup>, and Sr<sup>2+</sup>, and the stability of [Ba(tmec12)]<sup>2+</sup> more closely approaching that of [Ba(thec12)]<sup>2+</sup> where steric crowding is less significant in the coordination of the larger Ba<sup>2+</sup> ion. The stabilities of the alkaline earth complex ions in water are greater than those of the alkali metal analogues<sup>9</sup> where log(*K*/dm<sup>3</sup> mol<sup>-1</sup>) ≤ 2 is consistent with the greater electrostatic interaction of the divalent metal ions with the ligand increasing stability.

**Eight-Coordinate [M(thec12)]<sup>2+</sup> and [M(tmec12)]<sup>2+</sup> Enantiomerization.** The low freezing point of methanol-<sup>12</sup>C-*d*<sub>4</sub> permits a detailed study of the temperature dependence of the <sup>13</sup>C NMR spectra of the [M(thec12)]<sup>2+</sup> and [M(tmec12)]<sup>2+</sup> Mg<sup>2+</sup>, Ca<sup>2+</sup>, and Ba<sup>2+</sup> complexes that encompass the larger alkaline earth ions. Under slow-exchange conditions at 199.4 K in methanol-<sup>12</sup>C-*d*<sub>4</sub>, the <sup>13</sup>C NMR spectrum of [Mg(thec12)]<sup>2+</sup> consists of four resonances at 48.07 and 48.81 ppm assigned to the macrocyclic ring carbons *a* and *b*, which cannot be separately identified from these data, and 51.82 and 55.37 ppm assigned to the pendant arm >NCH<sub>2</sub>–, *c*, and –CH<sub>2</sub>OH, *d*, carbons, respectively (Figure 2). (The resonance labels *a*–*d* correspond to those used for the carbon atoms in Figure 1.) Four similarly assigned resonances at 48.46, 49.14, 54.01, and 56.02 ppm are observed at 199.4 K for [Ca(thec12)]<sup>2+</sup> and for [Ba(thec12)]<sup>2+</sup> at 48.44, 49.14, 55.73, and 56.66 ppm at 199.4 K. The <sup>13</sup>C NMR spectrum of [Ca(tmec12)]<sup>2+</sup> at 236.0 K consists of five resonances at 45.49 and 49.49 ppm assigned to the macrocyclic ring carbons *a* and *b* and 49.13, 58.88, and 67.53 ppm assigned to the pendant arm >NCH<sub>2</sub>–, *c*, –CH<sub>2</sub>OCH<sub>3</sub>, *e*, and –CH<sub>2</sub>OCH<sub>3</sub>, *d*, carbons, respectively. Five similarly assigned resonances at 45.91, 50.35 (*a* and *b*), 51.49 (*c*), 58.41 (*e*), and 67.83

- (9) Stephens, A. K. W.; Lincoln, S. F. *J. Chem. Soc., Dalton Trans.* **1993**, 2123–2126.  
 (10) Buøen, S.; Dale, J.; Krane J. *Acta Chem. Scand. B* **1984**, *38*, 773–778.  
 (11) Gans, P.; Sabatini, A.; Vacca, A. *J. Chem. Soc., Dalton Trans.* **1985**, 1195–1200.  
 (12) Lincoln, S. F. *Prog. React. Kinet.* **1977**, *9*, 1–91.

- (13) Burgess, J. *Metal Ions in Solution*; Ellis Horwood Ltd.: Chichester, U.K., 1978; Chapter 7.  
 (14) Shannon, R. D. *Acta Crystallogr., Sect. A: Cryst. Phys. Diffr., Theor. Gen. Crystallog.* **1976**, *A32*, 751–767.

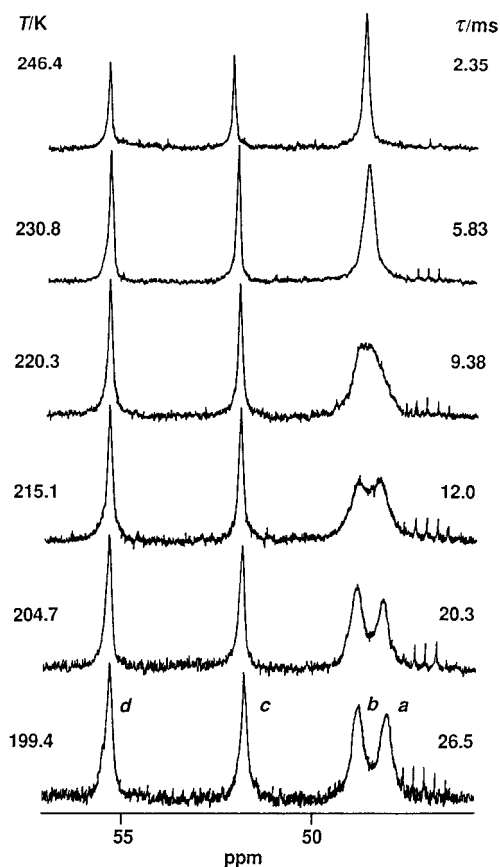


**Figure 2.** Temperature variation of the  $^{13}\text{C}$  NMR spectrum (75.47 MHz) of  $0.10 \text{ mol dm}^{-3}$   $[\text{Mg}(\text{thecl2})]^{2+}$  in methanol- $^{12}\text{C}-d_4$ . Experimental temperatures and  $\tau$  values derived from complete line shape analyses of the coalescing doublet arising from the macrocyclic ring methylene carbons, *a* and *b*, appear to the left and right of the figure, respectively. The resonances arising from the pendant arm  $-\text{NCH}_2-$ ,  $-\text{OCH}_3$ , and  $-\text{OCH}_2-$  are labeled *c*, *d*, and *e*, respectively.

(*d*) ppm are observed for  $[\text{Ba}(\text{tmec12})]^{2+}$  at 215.0 K. These slow-exchange spectra are consistent with all four pendant arms in  $[\text{M}(\text{thecl2})]^{2+}$  and  $[\text{M}(\text{tmec12})]^{2+}$  being equivalent on the  $^{13}\text{C}$  NMR time scale and eight-coordination of  $\text{M}^{2+}$ . (The  $^{13}\text{C}$  NMR spectrum of *tmec12* exhibits the pendant arm  $>\text{NCH}_2-$ ,  $-\text{CH}_2\text{OCH}_3$ , and  $-\text{CH}_2\text{OCH}_3$  resonances at 53.96, 56.77, and 69.42 ppm, respectively, at 210 K that show small variations in  $\delta$  with change in temperature, but the macrocyclic ring resonance at 50.18 ppm does not resolve into a doublet down to the freezing point.)

In each case the two macrocyclic resonances, *a* and *b*, broaden and coalesce with increase in temperature as the methylene carbons exchange with increasing rapidity between different magnetic environments in  $[\text{Mg}(\text{thecl2})]^{2+}$  (Figure 2) and its  $\text{Ca}^{2+}$  and  $\text{Ba}^{2+}$  analogues and in  $[\text{Ca}(\text{tmec12})]^{2+}$  and its  $\text{Ba}^{2+}$  analogue. However, the pendant arm resonances, *d*–*f*, only narrow slightly as temperature increases and viscosity decreases and show no effects arising from a chemical exchange process. This is consistent with exchange occurring between the distorted cubic  $\Lambda$  and  $\Delta$  enantiomers shown in Figure 1. At each temperature studied, complete line shape analyses of the coalescing doublets yielded the mean site lifetime,  $\tau$ , of the macrocyclic ring carbons in environment *a* or *b* that is related to the rate parameters in Table 2 through

$$1/\tau = k = (k_p T/h) \exp(-\Delta H^\ddagger/RT + \Delta S^\ddagger/R) \quad (1)$$

The  $\tau$  (ms) values were determined in the temperature range

where the exchange-induced resonance modifications are substantial, as shown in Figure 2 for  $[\text{Mg}(\text{thecl2})]^{2+}$ , and are 26.5 (199.4), 20.3 (204.7), 15.4 (209.9), 12.0 (215.1), 9.38 (220.3), 7.12 (225.5), 5.83 (230.8), 4.37 (236.0), and 2.35 (246.4) and 153 (225.5), 73.8 (236.0), 54.5 (241.2), 25.6 (251.6), 18.2 (256.9), 12.9 (262.1), 9.09 (267.3), 6.67 (272.5), 4.88 (277.7), and 2.11 (293.4) for  $[\text{Ca}(\text{thecl2})]^{2+}$  and 106 (246.4), 44.4 (256.9), 20.0 (267.3), 13.8 (272.5), 9.34 (277.7), 6.25 (283.0), 4.08 (288.2), 3.03 (293.4), 2.04 (299.1), 1.59 (304.4), 0.83 (315.0), and 0.61 (320.3) for  $[\text{Ba}(\text{thecl2})]^{2+}$ , where the corresponding temperatures (K) appear in parentheses. The analogous data are 125 (256.9), 44.4 (267.3), 17.2 (277.7), 10.6 (283.0), 7.14 (288.2), 4.55 (293.8), 2.78 (299.1), 2.02 (304.4), 1.43 (309.7), 0.95 (315.0), 0.67 (320.3), 0.46 (325.6), and 0.33 (331.0) for  $[\text{Ca}(\text{tmec12})]^{2+}$  and for  $[\text{Ba}(\text{tmec12})]^{2+}$  are 1000 (215.1), 333 (225.5), 125 (236.0), 50.0 (246.4), 21.7 (256.9), 14.7 (262.1), 10.0 (267.3), 6.90 (272.5), 5.00 (277.7), 3.64 (283.0), 2.63 (288.2), 1.89 (293.8), 1.43 (299.1), 1.05 (304.4), 0.77 (309.7), 0.59 (315.0), 0.44 (320.3), 0.34 (325.6), and 0.27 (331.0).

A substantial variation in  $\Delta H^\ddagger$  and  $\Delta S^\ddagger$  occurs for the five eight-coordinate complexes in Table 2, but no obvious trend emerges other than that  $\Delta S^\ddagger$  is negative in each case. Each enantiomerization requires inversion at each nitrogen as the transition state is approached, and this may lead to a stiffer structure consistent with a negative  $\Delta S^\ddagger$ . However, such a conclusion must be viewed with caution as it is not known to what extent metal center–ligand bond breaking is involved in the enantiomerization and which step in the sequential process is characterized by the activation parameters. Nevertheless, it is clear that the enantiomerization mechanism is intramolecular as intermolecular ligand exchange occurs much more slowly than enantiomerization as is discussed below.

**Seven-Coordinate  $[\text{Mg}(\text{tmec12})]^{2+}$  Exchange.** The  $^{13}\text{C}$  NMR spectral temperature variation of  $[\text{Mg}(\text{tmec12})]^{2+}$  (Figure 3) differs markedly from those of its  $\text{Ca}^{2+}$  and  $\text{Ba}^{2+}$  analogues. It shows coalescence to singlets (280.8 K) of the slow-exchange multiplet (187.1 K) of the pendant arm  $>\text{NCH}_2-$ , *e*–*g*, and that of the macrocyclic ring, *a*–*d*, that overlap in the range 46–55 ppm. It also shows a narrowing of the broadened singlet, *h*–*j*, for  $-\text{OCH}_3$  at 57.5 ppm with increase in temperature and a coalescence to a singlet (280.8 K) of the triplet, *k*–*m*, for  $-\text{OCH}_2-$  at 66–70 ppm observed in slow exchange (187.1 K). This is consistent with  $[\text{Mg}(\text{tmec12})]^{2+}$  being seven-coordinate and with increased steric crowding over that in  $[\text{Mg}(\text{thecl2})]^{2+}$  causing the decrease in coordination number from 8 to 7.

The  $^{13}\text{C}$  NMR spectral temperature variation may be interpreted through the exchange scheme shown in Figure 4, where the  $^{13}\text{C}$  resonance labels alluded to above are the same as those assigned to individual carbon atoms in Figure 4. The  $-\text{OCH}_2-$  triplet has an approximate area ratio 1:1:2 consistent with three different environments, *k*, *m*, and *l*, in seven-coordinate  $[\text{Mg}(\text{tmec12})]^{2+}$  (Figure 5), and its coalescence may be analyzed through the scheme in Figure 4. Either the *random* process operates where all of the exchange paths between A and D are followed or the *sequential* process operates where exchange occurs between adjacent pendant arms only in the sequence  $\text{A} \rightarrow \text{B} \rightarrow \text{C} \rightarrow \text{D}$  and its reverse. Three-site exchange, assuming identical exchange probabilities between adjacent and diagonal pendant arms in the *random* process, produces the best fit coalescence spectral variation shown in Figure 5. The  $\tau$  (ms) values determined in the temperature range where the exchange-induced resonance modifications are substantial, and where the values in parentheses are the corresponding temperatures (K),

**Table 2.** Kinetic Parameters for Intramolecular Exchange in  $[\text{M}(\text{thec12})]^{2+}$  and  $[\text{M}(\text{tmec12})]^{2+}$  in Methanol- $^{12}\text{C}-d_4$ 

complex	$k^a/\text{s}^{-1}$	$k(298.2\text{ K})/\text{s}^{-1}$	$\Delta H^\ddagger/\text{kJ mol}^{-1}$	$\Delta S^\ddagger/\text{J K}^{-1}\text{ mol}^{-1}$
$[\text{Mg}(\text{thec12})]^{2+}$	$85 \pm 3 (215.1)$	$2310 \pm 260$	$19.1 \pm 0.8$	$-117 \pm 4$
$[\text{Ca}(\text{thec12})]^{2+}$	$80 \pm 1 (262.1)$	$582 \pm 17$	$33.3 \pm 0.5$	$-80.3 \pm 1.8$
$[\text{Ba}(\text{thec12})]^{2+}$	$112 \pm 1 (277.7)$	$445 \pm 5$	$43.9 \pm 0.4$	$-47.0 \pm 1.3$
$[\text{Mg}(\text{tmec12})]^{2+ b}$	$610 \pm 10 (218.4)$	$163\,000 \pm 8000$	$35.8 \pm 0.4$	$-25.1 \pm 1.7$
$[\text{Ca}(\text{tmec12})]^{2+}$	$494 \pm 2 (304.4)$	$310 \pm 1$	$54.0 \pm 0.2$	$-16.1 \pm 0.5$
$[\text{Ba}(\text{tmec12})]^{2+}$	$724 \pm 3 (299.1)$	$688 \pm 3$	$39.6 \pm 0.1$	$-57.9 \pm 0.3$

<sup>a</sup> Rate constant at temperature near coalescence shown in parentheses. <sup>b</sup> These data refer to pendant arm exchange.

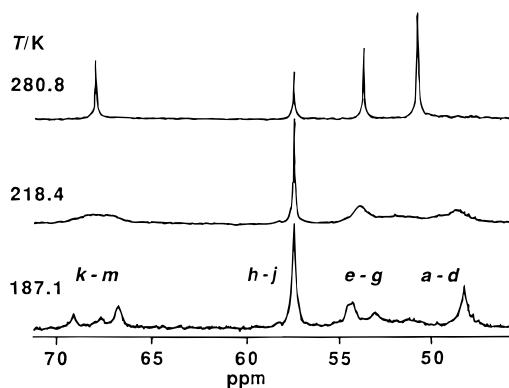


**Figure 3.** Temperature variation of the  $^{13}\text{C}$  NMR spectrum (75.47 MHz) of  $0.10\text{ mol dm}^{-3}$   $[\text{Mg}(\text{tmec12})]^{2+}$  in methanol- $^{12}\text{C}-d_4$ . Experimental temperatures appear to the left of the figure. The macrocycle resonances are labeled *a-d*, the pendant arm  $-\text{NCH}_2-$  resonances, *e-g*, the  $-\text{OCH}_3$  resonances, *h-j*, and the  $-\text{OCH}_2-$  resonances, *k-m*.

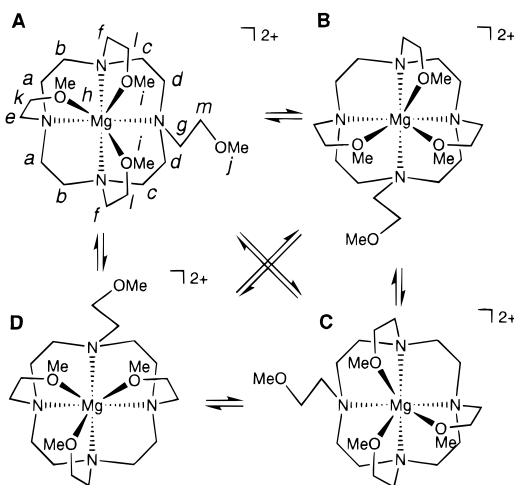


**Figure 4.** Mechanism proposed for intramolecular exchange on  $[\text{Mg}(\text{tmec12})]^{2+}$ .

are 51.7 (187.1), 25.0 (192.4), 13.9 (197.6), 8.20 (202.8), 5.00 (208.0), 3.03 (213.2), 1.82 (218.4), 0.95 (222.6), 0.61 (228.8), 0.41 (234.1), 0.27 (239.3), 0.18 (244.5), and 0.12 (249.7). The derived activation parameters appear in Table 2. Using the  $\tau$  values derived through the *random* process to generate the spectral variation resulting from the *sequential* process produces spectra (Figure 5) that resemble the experimental spectra less closely than those arising from the *random* process. Thus, the random exchange process dominates the temperature spectral variation of seven-coordinate  $[\text{Mg}(\text{tmec12})]^{2+}$ .

Intermolecular *tmec12* exchange on  $[\text{Mg}(\text{tmec12})]^{2+}$  in a methanol- $^{12}\text{C}-d_4$  solution where  $[\text{Mg}(\text{tmec12})]^{2+}$  and  $[\text{tmec12}]_{\text{free}}$  were both  $0.050\text{ mol dm}^{-3}$  is characterized by  $k(298.2\text{ K}) = 29800 \pm 800\text{ s}^{-1}$ ,  $\Delta H^\ddagger = 61.7 \pm 0.4\text{ kJ mol}^{-1}$ , and  $\Delta S^\ddagger = 47.7$

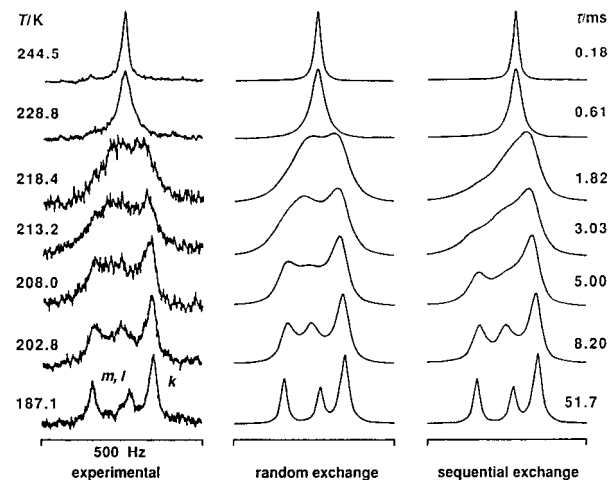


**Figure 5.** Temperature variation of the  $^{13}\text{C}$  NMR spectrum (75.47 MHz) of the  $-\text{OCH}_2-$  resonances (*k-m*) arising from a  $0.10\text{ mol dm}^{-3}$   $[\text{Mg}(\text{tmec12})]^{2+}$  solution in methanol- $^{12}\text{C}-d_4$ . Experimental temperatures appear to the left of the figure. The  $\tau$  values derived from complete line shape analyses of the coalescing triplet arising from the pendant arm  $-\text{OCH}_2-$  according to the random process appear to the right of the figure, and these values were used to generate the line shapes expected for the sequential process.

$\pm 1.5$  as determined from a complete line shape analysis of the coalescence of the  $-\text{OCH}_2-$  resonances of  $[\text{Mg}(\text{tmec12})]^{2+}$  and free *tmec12*. While this intermolecular exchange process is much slower than the intramolecular exchange process, both are much faster than those occurring in eight-coordinate  $[\text{Ca}(\text{tmec12})]^{2+}$  and  $[\text{Ba}(\text{tmec12})]^{2+}$  under the same conditions where no broadening of their  $-\text{OCH}_2-$  resonances and that of free *tmec12* occurs close to the solution boiling point. Neither is broadening of the  $-\text{OCH}_2-$  resonances of  $[\text{Mg}(\text{thec12})]^{2+}$  nor those of its  $\text{Ca}^{2+}$  and  $\text{Ba}^{2+}$  analogues and that of free *thec12* observed under similar conditions. Evidently the free pendant arm in  $[\text{Mg}(\text{tmec12})]^{2+}$  labilizes both the intra- and intermolecular exchange processes.

In several oxygen donor solvents the rate of solvent exchange is sufficiently slow for the occupancy of the first coordination sphere to be assigned by NMR methods that have shown  $[\text{Mg}(\text{H}_2\text{O})_6]^{2+}$  and  $[\text{Mg}(\text{CH}_3\text{OH})_6]^{2+}$  to be the greatly predominant species in their respective solvents.<sup>15,16</sup> The observation of eight- and seven-coordination in  $[\text{Mg}(\text{thec12})]^{2+}$  and  $[\text{Mg}(\text{tmec12})]^{2+}$ , respectively, is consistent with octadentate *thec12* and *tmec12* increasing the coordination number of  $\text{Mg}^{2+}$  through chelation.

**Acknowledgment.** Funding of this study by the Australian Research Council and the award of an Australian Postgraduate Research Award to A.K.W.S. are gratefully acknowledged.

**Supporting Information Available:** Figures S1 and S2, showing the temperature variations of the  $^{13}\text{C}$  NMR spectra (75.47 MHz) of  $0.10\text{ mol dm}^{-3}$   $[\text{Ba}(\text{thec12})]^{2+}$  and  $[\text{Ca}(\text{tmec12})]^{2+}$ , respectively, in methanol- $^{12}\text{C}-d_4$ . This material is available free of charge via the Internet at <http://pubs.acs.org>.

(15) Lincoln, S. F. *Coord. Chem. Rev.* **1971**, *6*, 309–329.

(16) Lincoln, S. F.; Merbach, A. E. *Adv. Inorg. Chem.* **1995**, *42*, 1–87.